




Development of a Nanostructured Film Containing Palygorskite and Dermaseptin 01 Peptide for Biotechnological Applications

Karla Costa Bezerra Fontenele Oliveira · Emanuel Airton de Oliveira Farias · Paulo Ronaldo Sousa Teixeira · Vitor Schwenck Brandão · Rafael Miguel Sábio · Alyne Rodrigues de Araújo · Peter Eaton · Luiz Carlos Bertolino · Marcelo Porto Bemquerer · Hernane da Silva Barud · José Roberto de Souza de Almeida Leite · Carla Eiras 

Accepted: 5 October 2023 / Published online: 9 November 2023
© The Author(s), under exclusive licence to The Clay Minerals Society 2023

Abstract Clay minerals are suitable matrices to anchor organic molecules such as antimicrobial peptides (AMPs) so that their bioactivity is maintained, enabling the formation of new materials with potential for new applications in biotechnology. The objective of the present study was to develop a nanostructured film where the properties of palygorskite (Plg) were combined at the molecular level with Dermaseptin 01 (DRS 01), in which the clay mineral also served as a substrate for the immobilization of this peptide. The films were prepared using the Layer-by-Layer (LbL) self-assembly technique. Crude palygorskite without purification (Plg IN) was subjected

to physical and chemical procedures to increase its adsorptive properties. The structure, chemical composition, and morphology of Plg were investigated by X-ray diffraction (XRD), Fourier-transform infrared spectroscopy (FTIR), X-ray fluorescence spectrometry (XRF), scanning electron microscopy (SEM), and transmission electron microscopy (TEM). LbL films were adsorbed onto ITO (Indium Tin Oxide) and characterized electrochemically by cyclic voltammetry (CV), UV-Visible spectroscopy, and atomic force microscopy (AFM). For the ITO/DRS 01 and ITO/Plg/DRS 01 films, an oxidation process at +0.77 V was observed, confirming that the DRS 01 maintained

Associate Editor: Jana Madejová.

K. C. B. F. Oliveira · E. A. d. O. Farias · P. R. S. Teixeira · C. Eiras (✉)

Laboratório de Pesquisa e Desenvolvimento de Novos Materiais e Sistemas Sensores (MATSENS), Universidade Federal do Piauí, Teresina, Piauí 64049-550, Brazil
e-mail: carla.eiras.ufpi@gmail.com

V. S. Brandão · L. C. Bertolino
Centro de Tecnologia Mineral – CETEM, Cidade Universitária, Ilha do Fundão, Rio de Janeiro, RJ 21941908, Brazil

R. M. Sábio · H. da Silva Barud
Laboratório de Biopolímeros e Biomateriais – BIOPOLMAT, Universidade de Araraquara, UNIARA, Araraquara, SP 14801320, Brazil

A. R. de Araújo · C. Eiras
Núcleo de Pesquisa em Biodiversidade e Biotecnologia – BIOTEC, Universidade Federal do Piauí, Campus Ministro Reis Velloso, Parnaíba, PI 64202020, Brazil

P. Eaton
LAQV-REQUIMTE, Departamento de Química e Bioquímica, Faculdade de Ciências da Universidade do Porto, 4169007 Porto, Portugal

M. P. Bemquerer
Embrapa Recursos Genéticos e Biotecnologia, Asa Norte, Brasília, DF 70770917, Brazil

J. R. de Souza de Almeida Leite
Faculdade de Medicina, FM, Universidade de Brasília, UnB, Campus Universitário Darcy Ribeiro, Brasília, DF 70910900, Brazil

its electroactive behavior and intrinsic properties. The results also showed that Plg served as excellent support for the immobilization of DRS 01, increasing its concentration and availability in the film form. This work reported immobilizing the DRS 01 peptide with Plg for the first time in an ultrathin film with bioactive properties. Thus, the film developed can be explored for applications such as biosensor devices and antimicrobial coating materials as well as other biotechnological applications.

Keywords Cationic antimicrobial peptides · Fibrous clay minerals · Layer-by-layer · *Pithecopus hypochondriasis* · Thin film

Introduction

Clay minerals are a class of inorganic material and are used widely in traditional medicine (Bourgeois, 2006; Carretero, 2002; Carretero et al., 2006; Iborra & González, 2006) with several industrial applications (Anirudhan & Ramachandran, 2007; Bergaya et al., 2006; Baltar et al., 2009; Liu et al., 2008; Madyan et al., 2017; Xavier et al., 2016;). Among their physicochemical characteristics are significant surface reactivity, ion exchange, adsorption, colloidal and dispersion capabilities, rheological properties, and low toxicity. Such features make them suitable for use as biomaterials, including excipients or active ingredients in pharmaceutical formulations, cosmetics (Carretero, 2002), drug carriers (Kim et al., 2016; López-Galindo et al., 2007), regenerative medicine (Chrzanowski et al., 2013; Ghadiri et al., 2015), and development of advanced materials, such as nanocomposites (Alcântara et al., 2015; Ruiz-Hitzky & Van Meerbeek 2006; Ruiz-Hitzky et al., 2013).

Palygorskite (Plg) is a raw 2:1 phyllosilicate with the approximate structural formula $\text{Si}_8\text{O}_{20}(\text{Al}_2\text{Mg}_2)(\text{OH})_2(\text{OH}_2)_4 \cdot 4\text{H}_2\text{O}$ (García-Romero et al., 2004) belonging to a nanofibrous group of clay minerals. The fiber-forming nature, resulting from the 180° inversion that occurs at every four tetrahedra of silicon, leads to the formation of a structure in open channels parallel to its central octahedral axis. This conformation is responsible for its adsorptive properties and large specific surface area, making it a suitable candidate to host bioactive molecules (Carazo et al., 2018; Lopéz-Galindo

et al., 2007; Romero & Barrios, 2008; Tajeu et al., 2018). One of the advantages of fibrous clay minerals, when compared to layered ones, is the silanol groups located on the outer surface and their negative charges which act as centers of interaction with polysaccharides such as chitosan, proteins, lipids, nucleic acids, enzymes, and amino acids (Alcântara et al., 2012; Alcântara et al., 2014, 2015; An et al., 2015; Benteoli et al., 2007; Castro-Smirnov et al., 2017; Huang et al., 2009; Mbougouen et al., 2006, 2007; Ruiz-Hitzky et al., 2013; You et al., 2011; Zaia, 2004;).

Numerous factors justify the use of Plg in devices. As Chen and Jin (2010) reported, Plg has a moderate absorptive capacity, good biological affinity, and a role in enhancing the accessibility of bioactive sites. Plg is a suitable immobilization matrix to prevent the protein structures (e.g. enzymes) from unfolding, resulting in high detective sensitivity during electrochemical sensing (Wu et al., 2011). However, despite the potential of Plg associated with biomolecules in the design of nanostructured systems, no study involving antimicrobial peptides (AMPs) has been reported.

AMPs correspond to a class of biomolecules isolated from various living organisms as part of the innate immune system. Their potential as new antibiotic molecules is firmly established in the literature as drug candidates (Chu et al., 2015; Ntwasa, 2012). Research involving AMPs has demonstrated their high activity in the micromolar concentration with a broad spectrum against bacterial pathogens (Mor et al., 1994), fungi (Leite et al., 2008), viruses (Belaid et al., 2002), protozoa (Brogden & Brogden, 2011; Calderon et al., 2009; Moraes et al., 2011a, 2011b), and cancer cells (Buri et al., 2011; Chu et al., 2015; Gaspar et al., 2013).

Dermaseptin 01 (DRS 01) (Amiche et al., 2008) is a peptide isolated from the cutaneous secretion of South American amphibians of the genus *Pithecopus* (Cope, 1866). DRS 01 has been the subject of many studies since its discovery, including its association with nanostructures (Bittencourt et al., 2016; Brand et al., 2002, 2006, 2013; Castiglione-Morelli et al., 2005; Eaton et al., 2014; Leite et al., 2008; Moraes et al., 2011a, 2011b, 2013; Salay et al., 2011; Silva et al., 2008; Zampa et al., 2009). Recent research has focused on strategies for the modification of AMPs, including hybrid, stabilized, or immobilized

AMPs using various materials, allowing innovations in the applications due to increased stability or even the enhancement of previously existing properties (Brogden & Brogden, 2011; Costa et al., 2011; Onaizi & Leong, 2011). Because of their biological activity, AMPs can be used as recognition elements when interacting with target substances through intermolecular reactions in sensor devices or as coating agents (Lillehoj et al., 2014; Plácido et al., 2016; da Silva et al., 2014).

Electrochemical sensors are among the most widely used chemical sensors due to their selectivity, sensitivity, simplicity, and low cost. In this field, organic molecules immobilized on clay minerals may play an essential role in developing electrochemical sensors and biosensors as matrices for the adsorption of electroactive ions (Gianfreda et al., 2002; Mousty, 2004; Navrátilová & Kula, 2003). Aluminosilicates are materials of interest because of their hydrophilicity, porosity, and mechanical and thermal stability (Chen & Jin, 2010; Mousty, 2004; Navrátilová & Kula, 2003).

The production of functional films based on clay minerals is possible from nanometric dispersions in aqueous media (Chrzanowski et al., 2013; Ghadiri et al., 2015; Huang et al., 2008; Ruiz-Hitzky et al., 2013). Thus, clay minerals represent suitable materials for preparing nanostructured composites associated with AMPs in the search for new materials for use in biotechnology. Thus, the layer-by-layer (LbL) self-assembly technique enables the formation of thin films where the properties of Plg and DRS 01, for example, can be combined and explored at a molecular level. These films can be used in several areas, e.g. as electrochemical sensors, as biomolecule-delivery systems, and as functional coatings (Decher, 1997; Decher & Schlenoff, 2012; Gentile et al., 2015; Kim et al., 2015; Lehn, 2007; Picart et al., 1998, 2015; Rawtani & Agrawal, 2014; Ruiz-Hitzky et al., 2013; Skorb et al., 2014).

Thus, the objective of the present study was to prepare nanostructured films where the properties of Plg are combined at the molecular level with DRS 01, serving as a support platform for immobilizing this peptide and improving its adoption and availability. The strategy proposed in this study led to the development of a new nanomaterial the applications of which can be explored in the vast biotechnology field.

Experimental

Preparation of Materials

Antimicrobial Peptide

DRS 01 (GLWSTIKQKGKEAAIAAA-KAA-GQAALGAL-NH₂) was synthesized by the 9-fluorenylmethoxycarbonyl (Fmoc) solid-phase strategy (Chan & White, 2000) as reported previously (Brogden, 2005). Reagents used for peptide synthesis were acquired from Peptides International (Louisville, Kentucky, USA). Purification was performed on a preparative reversed-phase column (RP) (Vydac 218 TP 510, Hesperia, California, USA) coupled to the HPLC system model LC-10VP (Shimadzu Corp., Kyoto City, Japan). The molecular weight (2793.39 Da) and sample purity were confirmed using MALDI-TOF/TOF mass spectrometry, as described by Bittencourt et al. (2016).

Palygorskite

Palygorskite (Plg) was collected from a deposit located in the Coimbra, Cardoso company mine (coordinates: 23 M064043 9,249,510; elevation: 185.7 m) in the municipality of Guadalupe, state of Piauí (northeast region of Brazil). The raw Plg was submitted to the beneficiation process, involving comminution and magnetic separation steps in a high-intensity field (14,000 Gauss) to remove iron (oxyhydr)oxides. The next stage was wet sieving in a 635# sieve (20 µm). The <20 µm fraction was purified by washing several times in distilled water and centrifuging. The precipitate was dried and treated with hydrogen peroxide (H₂O₂) in sodium acetate and acetic acid buffer under stirring at 45°C for 72 h; all the chemicals were obtained from Sigma Aldrich (St. Louis, Missouri, USA). Following further washings, the fine fraction was stored in a desiccator and used to produce LbL films. All the chemicals were of analytical quality and were used as supplied without further purification.

Preparation and Characterization of LbL Films

The ITO slides (A ≈ 0.40 cm²) were previously cleaned in detergent and deionized water (1:6, v:v) under heating until 75°C and, after that, sonicated

in acetone (purchased from Merck, São Paulo, Brazil) for 10 min. Subsequently, the RCA (Radio Corporation of America) protocol was used to hydrophilize the substrates in an alkaline medium (Kim et al., 1998) by adding deionized water, NH_4OH , and H_2O_2 (purchased from Merck) (5:1:1, v:v). The substrates were dipped in the RCA solution at 75–80°C for 30 min and then rinsed twice in deionized water. All substrates were then dried with a gentle N_2 flow. For the deposition of films, DRS 01 and Plg were first stored individually in 1.5 mL microtubes and dispersed in deionized water (pH 5.6, 25°C, resistivity of 18 M Ω cm). Both dispersions were used at the concentration of 1.0 mg mL⁻¹ and sonicated for 10 min to improve the dispersion of the material (Fernandes et al., 2009). In the case of Plg, this step was fundamental for obtaining nanoscale particles and improving their adsorption capacity (Wang & Wang, 2016). The immobilization was performed by alternating exposure of the ITO substrate to Plg and DRS 01, respectively, for 5 min, according to previous studies (Bittencourt et al., 2016; Zampa et al., 2009). Between immersions, the substrates were washed in deionized water to remove non-adsorbed molecules and dried with a gentle N_2 flow.

Palygorskite Characterization

XRD

X-ray diffraction of Plg was carried out using the powder method and the results collected using a Bruker D-4 Endeavor instrument (Billerica, Massachusetts, USA) with $\text{CuK}\alpha$ (40 kV/40 mA). The scans were conducted from 4 to 80°2 θ using a step size of 0.04°2 θ and a counting time of 2 s, using a Lynx Eye position-sensitive detector. Qualitative interpretations of the XRD patterns were compared using the standards in the database PDF02 (ICDD, 2006) in the Bruker software, *Diffraction^{Plus}*.

FTIR

Infrared spectra were obtained using KBr pellets in the region between 4000 and 400 cm⁻¹ with a Bruker Vector 3.3 FTIR spectrometer. A total of 96 scans was collected for each sample at 4 cm⁻¹ resolution.

XRF

The chemical composition of the Plg sample was determined using an Axios X-ray fluorescence spectrometer (Panalytical). The purified Plg sample was prepared in a Vaneox automatic press (20 mm template, P = 20 ton and t = 30 s), using boric acid (H_3BO_3) as the binder in the ratio of 1:0.3–0.6 g of acid and 2.0 g of the dried sample at 100°C. Semi-quantitative results (standardless) were expressed as %, calculated as oxides normalized to 100%.

SEM-EDS

Scanning electron microscopy and energy dispersive X-ray spectroscopy were performed using an FEI-Quanta FEG 250 SEM instrument (Thermo Fischer Scientific, Hillsboro, Oregon, USA). The samples were sputter coated with Au and imaged using both the secondary electron and backscattered electron modes.

Transmission Electron Microscopy (TEM)

The micrographs were obtained using a Philips CM 200 Super Twin Transmission Electron Microscope. The samples were prepared by dispersing the material in 2-propanol in microtubes submitted to an ultrasonic bath for 10 min. After fiber dispersion, a drop was deposited on a microscopy grid and dried before examination.

Film Characterizations

Cyclic Voltammetry (CV)

All measurements were performed in triplicate to ensure their reproducibility. The Plg/DRS 01 LbL films were characterized by CV in a Dropsens μStat 400 bipotentiostat/galvanostat instrument (Dropsens, Llanera, Spain) and an electrochemical cell with a capacity of 50 mL containing three electrodes. The reference electrode was a saturated calomel electrode (SCE) [$\text{Hg}/\text{HgCl}/\text{KCl}$ (sat.)], while a platinum plate ($A = 1.0 \text{ cm}^2$) was used as an auxiliary electrode. The LbL films deposited on the ITO electrode for ITO/Plg/DRS 01 sequence were used as the working electrodes. Potassium phosphate buffer ($\text{KH}_2\text{PO}_4/\text{K}_2\text{HPO}_4$), 0.1 M, pH 7.2 at 25°C, was used as an

electrolytic solution. The potential scanning rate was 50 mV s^{-1} .

Spectroscopy in the Ultraviolet-Visible Region (UV-Vis)

LbL films were characterized by UV-Vis spectroscopy employing an Agilent Cary 60 spectrophotometer (Santa Clara, California, USA) between 200 and 800 nm scanning. For the UV-Vis measurements, the Plg/DRS 01 film was adsorbed on a quartz substrate to probe peptide absorption in the ultraviolet region (216 and 280 nm). Successive spectra were recorded for each adsorbed bilayer until the stable growth of the LbL film was observed.

AFM

AFM was used to evaluate the surface roughness of the ITO/Plg and ITO/Plg/DRS 01 films and the ITO clean substrate. Images were collected at 512-pixel resolution in tapping mode on a TT-AFM instrument (AFM Workshop, Signal Hill, California, USA). Representative images were examined using ACT-20 (AppNano, Mountain View, California, USA) silicon tip cantilevers with radius $<10 \text{ nm}$ with a resonance frequency of $\sim 353 \text{ kHz}$. Three areas of each sample

were examined. The images were analyzed using *Gwyddion 2.4* software. All roughness results were expressed as mean \pm SD. To compare the average roughness (R_a values) of surfaces in the LbL films, an analysis of variance (ANOVA) was performed. Statistical analyses were performed using *GraphPad Prism® 6.0* software, and a $p < 0.05$ value was considered statistically significant.

Results and Discussion

XRD Analysis of Plg

The X-ray patterns of Plg in the non-magnetic $<20 \mu\text{m}$ fraction and purified Plg were obtained after the chemical treatment (Fig. 1). The results indicated that the sample consisted mainly of palygorskite and, secondarily, kaolinite and quartz were identified with the help of crystallographic data sheets for both samples (JCPDF No. 31-0783, 1-830971, and 1-791910).

The XRD region of Plg with the highest reflection intensity was at $\sim 8.6^\circ 2\theta$ (Sheng & Wang, 2005), which corresponded to $d_{110} = 1.05 \text{ nm}$ attributed to the basal plane in the Plg structure (Bailey, 1980; Oliveira et al., 2013; da Silva et al., 2013).

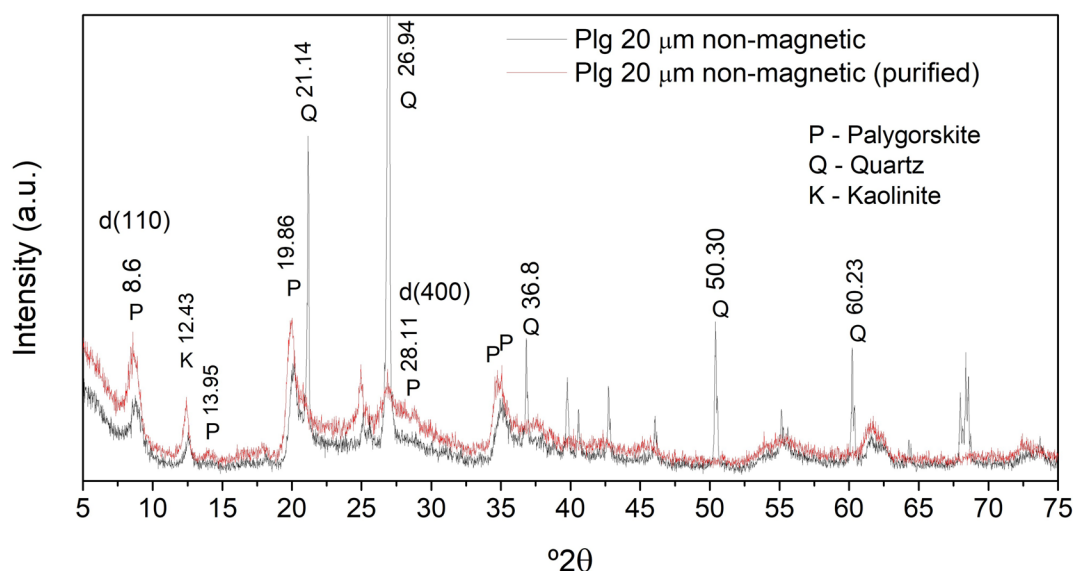


Fig. 1 XRD patterns of non-magnetic $<20 \mu\text{m}$ and purified non-magnetic $<20 \mu\text{m}$ clay samples. $\text{CuK}\alpha$ (40 kV/40 mA). The letters above each peak are assignments of the origin (see legend)

Other reflections characteristic of this clay material were also identified at 13.95, 19.86, and 28.11°2 θ for the (200), (040), and (400) reflections, respectively. The diffraction next to 27.00°2 θ is associated with the presence of quartz.

X-ray diffraction of the purified sample revealed an increase in the characteristic intensity of Plg attributed to the (110) reflection, which is of greater intensity than the quartz reflection. This evidence suggests a high purity obtained by complementing the 635# mesh screening techniques with washing and centrifugation of the raw Plg.

FTIR Results of Plg

The bands in the FTIR spectra (Fig. 2) were divided into the stretching vibrations of structural O-H and adsorbed water and the O-H bending vibrations in the microchannels or “zeolitic” water (Murray, 2007; Suárez & García-Romero, 2006a).

The band at 3686 cm⁻¹ (Fig. 2) is attributed to the stretching vibrations of octahedral Mg₃-OH groups (Cai et al., 2007; Yan et al., 2012). The 3616 cm⁻¹ and 912 cm⁻¹ bands are attributed to the octahedral Al₂-OH stretching and deformation modes, respectively (Suárez & García-Romero, 2006a). Although the band positions in the two Plg samples were similar, the greater intensity of the band at 3616 cm⁻¹ in the purified sample confirmed the XRD results.

A low-intensity band at 3580 cm⁻¹ was attributed to Al-OH-Fe³⁺ stretching (Suárez & García-Romero,

2006a) and the band at 3550 cm⁻¹ can be attributed to the octahedral OH-Fe³⁺ stretching (Yan et al., 2012). By the results of Suárez & García-Romero (2006b), the band at 3431 cm⁻¹ appeared more clearly after the purification of the Plg, which can be attributed to the stretching of hydroxyls in the adsorbed water molecules. The band at 3390 cm⁻¹ originates from intramolecular hydrogen bonding of OH with Al-Fe³⁺ or Al-Mg groups in the Plg structure (Xavier et al., 2016; Suárez & García-Romero 2006a, 2006b). According to Madejová and Komadel (2001), the bands at 1006 and 1028 cm⁻¹ can be attributed to the Si-O vibrational stretching in the plane and 1114 cm⁻¹ in the Si-O stretching vibrations in the plane (longitudinal mode).

The band at 834 cm⁻¹ appeared only in the purified sample. According to Suárez and García-Romero (2006a), it belongs to Al-Mg-OH bending, indicating that Mg²⁺, for this sample, may occupy the M2 sites in the octahedral sheet. However, as observed by Chahi et al. (2002), the low intensity of this band casts doubt on this suggestion.

The band at 647 cm⁻¹, according to Yan et al. (2012), consists of a characteristic vibration of the Plg related to its channel structure. As stated by Cai et al. (2007), in samples poor in Mg²⁺, as is the case for the Plg sample in this study, this band is attributed to Fe³⁺-OH groups.

Impurities in the samples may account for the FTIR bands at 798 and 778 cm⁻¹, typical of symmetrical quartz stretching vibrations (Si-O-Si), as reported

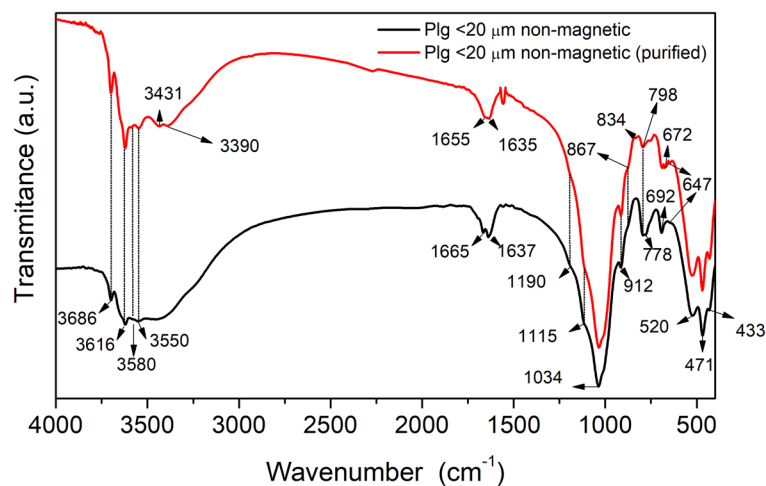


Fig. 2 FTIR spectra in the 4000–400 cm⁻¹ region of non-magnetic <20 μm and purified non-magnetic samples

by Suárez and García-Romero (2006a) and Yan et al. (2012). The first band showed a visible reduction in the purified sample, while the latter disappeared, corroborating the XRD results.

XRF Analysis of Plg

The chemical composition (wt.%) of the purified Plg was obtained by XRF analysis (Table 1), which identified the main oxides present in the sample. The results obtained by XRF indicated that SiO₂ and Al₂O₃ are the main constituents of the sample and that the Al content is greater than Si. This result also indicated that the Plg is of type I, according to the classification proposed by Suárez et al. (2007), giving it a dioctahedral character in which the octahedral sheet is occupied primarily by Al, with lesser Mg (20.4% Al₂O₃ and 3.9% MgO). These results agreed with those of Belaroui et al. (2014).

As Suárez and García-Romero (2006a) stated, the use of the chemical composition data obtained by XRF to determine the di- or trioctahedral character of the Plg can be checked by comparing with the FTIR spectra. The position and intensity of the band at 3616 cm⁻¹ is more consistent with Al₂-OH than with Mg₃-OH and, thus, indicates that the Plg is primarily dioctahedral.

Because the sample was subjected to magnetic separation, the remaining amount of iron consisted mostly of structural octahedral Fe³⁺. Stucki (2006) stated that removing separate iron oxide phases by chemical means without some alteration in the remaining phases is unlikely. An advantage of the magnetic separation technique is that it does not alter the constituents in the clay mineral structure, as occurs with chemical processes.

Morphology Analysis of Plg by SEM and TEM

The morphology and porosity of the purified Plg were evaluated by SEM (Fig. 3A,B) and TEM (Fig. 3C,D) measurements. SEM images displayed aggregates of

rods, usually formed by lath units scarcely visible at a magnification of <50,000×. According to the SEM images, several aggregated rods can form bundles of fibers, which has also been observed by others (García-Romero et al., 2013).

The TEM images (Fig. 3C,D) corroborated the SEM results, showing individual laths building up rods and, consequently, a group of rods. The laths in the rods showed a width <20 nm, which also agreed with previous works (Gan et al., 2009; García-Romero et al., 2013; Xavier et al., 2016). SEM and TEM analysis revealed lath lengths from 0.5 to 5 μm, confirming the formation of small- and medium-sized fibers (García-Romero et al., 2013). SEM and TEM images also displayed straight and rigid fibers without bending variation.

The texture composed of straight fibers oriented in all directions suggested high porosity and, generally, associated with an increase in surface area available for adsorbance modification and related applications (Suarez et al., 2013; García-Romero et al., 2013; Wang et al., 2016).

It is possible to verify that the bundle of fibers was formed by smaller fibers that can vary between 10 and 30 nm, corroborating with the studies by García-Romero and Suárez (2013). That corresponds to the crystal unit. When dispersed in solution and subjected to a sonication process, these fibers form a nanoscale network with advantageous properties such as large area and surface activity (Wang & Wang, 2016).

Electrochemical Studies of LbL Films Based on Plg and DRS 01

Cyclic voltammetry was used to verify the electrochemical behavior of the peptide associated with the clay mineral after deposition in the LbL film (Fig. 4). The CV was initially recorded for the unmodified ITO substrate. ITO was modified with a monolayer of DRS 01 or purified Plg conjugated to the antimicrobial peptide DRS 01 in bilayer film form (ITO/Plg/DRS 01). Aiming to verify the influence of the

Table 1 Chemical composition of purified Plg sample (wt.%)

Sample	SiO ₂	Al ₂ O ₃	Fe ₂ O ₃	MgO	K ₂ O	TiO ₂	Na ₂ O	CaO	MnO	*LOI
Purified Plg	53.0	20.4	9.0	3.9	2.5	0.56	0.36	0.29	0.11	9.4

* Loss on ignition

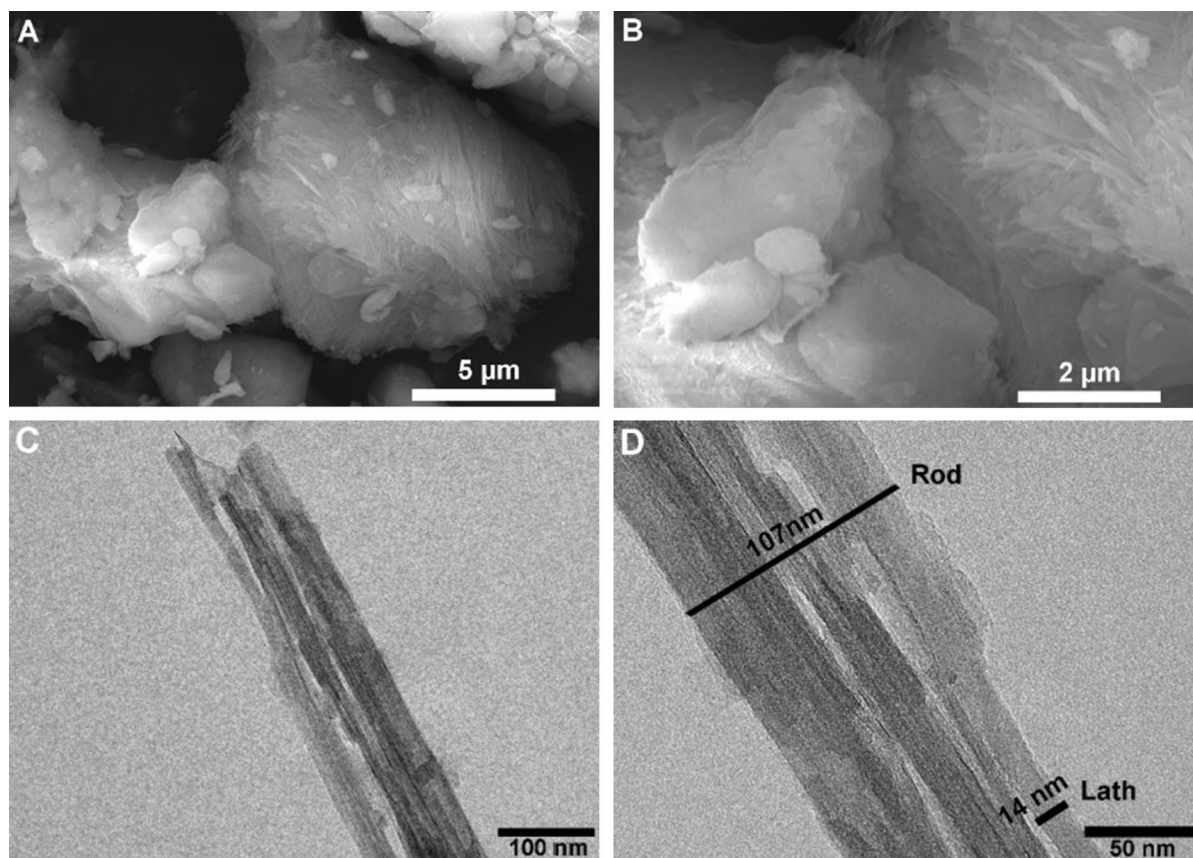


Fig. 3 SEM (A, B) and TEM (C, D) images of purified Plg

purification process on Plg, a film containing unpurified Plg (IN) (ITO/Plg-IN/DRS) was also obtained (Fig. 4). The unmodified ITO exhibited no redox reaction over the potential range from +0.5 to +1.0 V (vs SCE and $v = 50$ mV/s). However, the ITO modified with a DRS 01 monolayer film was oxidized at +0.77 V vs SCE, which is attributed to the electroactivity of the peptide due to the presence of tryptophan residues (Trp) (Plgeček, 2015).

The presence of the clay mineral in the ITO modified with bilayer films, i.e. ITO/Plg/DRS 01 or ITO/Plg-IN/DRS 01, notably neither blocked the electrode surface or interfered with the peptide response, which continued to be observed at the same potential (Fig. 4).

According to Murray (2007), Plg maintains its properties in the presence of electrolytes, without flocculation, because of the inhibition of sedimentation by the elongated crystals. In addition, when dispersed in water, fibrous clay minerals can

interconnect their fibers, creating an anchorage network for biomolecules. Studies showed that raw clay minerals are suitable for incorporation or immobilization of biological molecules (Huang et al., 2008, 2009; Zhao et al., 2011). The CV results suggest that DRS 01 and Plg maintained their integrity in the film system studied here.

Comparing the bilayer films (Fig 4.) revealed an increase in current density from $1.82 \mu\text{A cm}^{-2}$ for the film containing unpurified Plg (ITO/Plg-IN/DRS 01) to $2.63 \mu\text{A m}^{-2}$ in the film containing purified Plg (ITO/Plg/DRS 01). The results confirmed that removing impurities from Plg influences the electrochemical response of the bilayer film and, consequently, its application. In addition, these results corroborate those indicated by the XRD analysis. Thus, because of the improvement in the current signal, the film based on purified Plg was selected for subsequent studies.

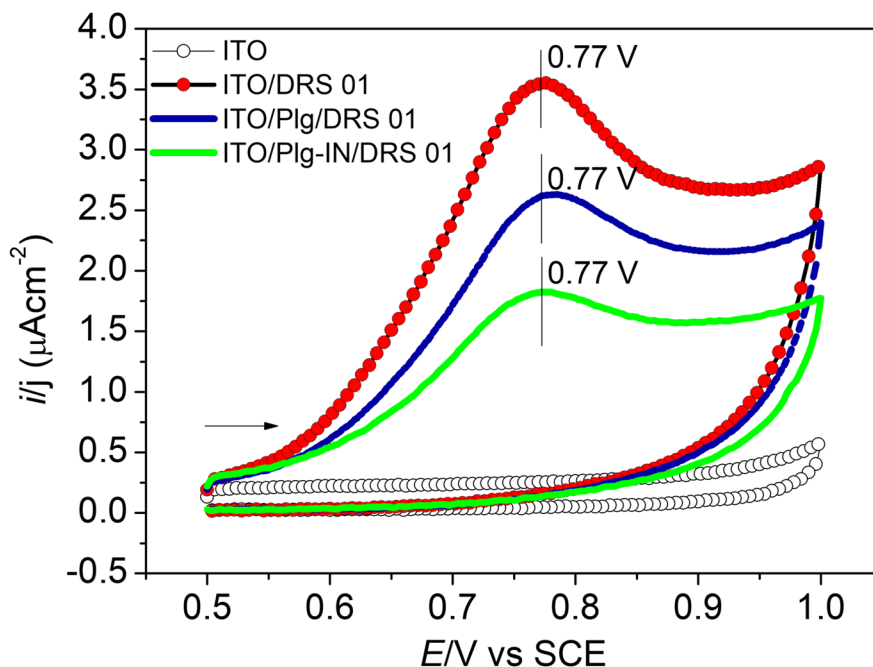


Fig. 4 Cyclic voltammograms of the unmodified ITO electrode (open circles), and ITO modified with DRS 01 monolayer film (ITO/DRS 01 - red), one bilayer of ITO/PIg/DRS 01 (blue), or ITO/PIg-IN/DRS 01 (green). All measurements were performed in 0.1 mol L^{-1} phosphate buffer, pH 7.5, at 50 mV s^{-1}

As stated by An et al. (2015), the large surface area of clay minerals exposes functional groups such as Si–O–Si, Si–OH, and Al(Mg)–OH, as well as hydrophobic groups in the tetrahedral sheet (hydroxyl groups) that can contribute to the interaction with organic molecules. For example, the hydrophilic portion of the octahedral surface interacts with the positively charged side chains of the proteins (Yu et al., 2013). Hydroxyl groups within the boundaries of tetrahedral and octahedral sheets are suitable for forming hydrogen bonds with enzymes, for example. In addition, van der Waal's forces play an essential role in binding proteins onto clay minerals and afford a partial overlap of the electrostatic repulsion (Yu et al., 2013). Therefore, other non-covalent interactions can occur between the PIg and AMPs and may govern the formation of the LbL films.

Previous studies into the anchoring of biomolecules on PIg (An et al., 2015; Basiuk et al., 1995; Benteoli et al., 2007) suggested that the conjugation with DRS 01 mainly occurs through electrostatic interactions, including hydrogen bonds, between the negatively charged clay surface (An et al., 2015) and the positively charged α -helical peptide

structure (Brand et al., 2006; Castiglione-Morelli et al., 2005). Furthermore, studies that investigated the adsorption of peptides and amino acids on the surfaces of silicates revealed a significant difference between the isoelectric point, e.g. for lysine (Lys) ($pI = 9.74$) and the point of zero charge for SiO_2 ($pzc = 2.8$) (Zaia, 2004; Parbhakar et al., 2007). Further studies are necessary to determine the secondary structure of DRS 01 ($pI = 10.0$) (Leite et al., 2008) bound to PIg. Bioactivity is required to explore AMPs as detection agents, and the present study allowed a perspective of the application of these films in areas such as clinical medicine, food safety, infection prevention, and environmental protection.

The next step of this study was to evaluate the influence of the number of deposited bilayers (n) on the electrochemical response of ITO/PIg/DRS 01 films (Fig. 5).

The three-bilayer film ITO/(PIg/DRS 01)₃ showed an increase in current density to $4.60 \mu\text{A cm}^{-2}$ (Fig. 4) compared to $2.54 \mu\text{A cm}^{-2}$ in the film with a single bilayer (Fig. 5). On the other hand, in the 5-bilayer film, the current density decreased to $3.71 \mu\text{A cm}^{-2}$.

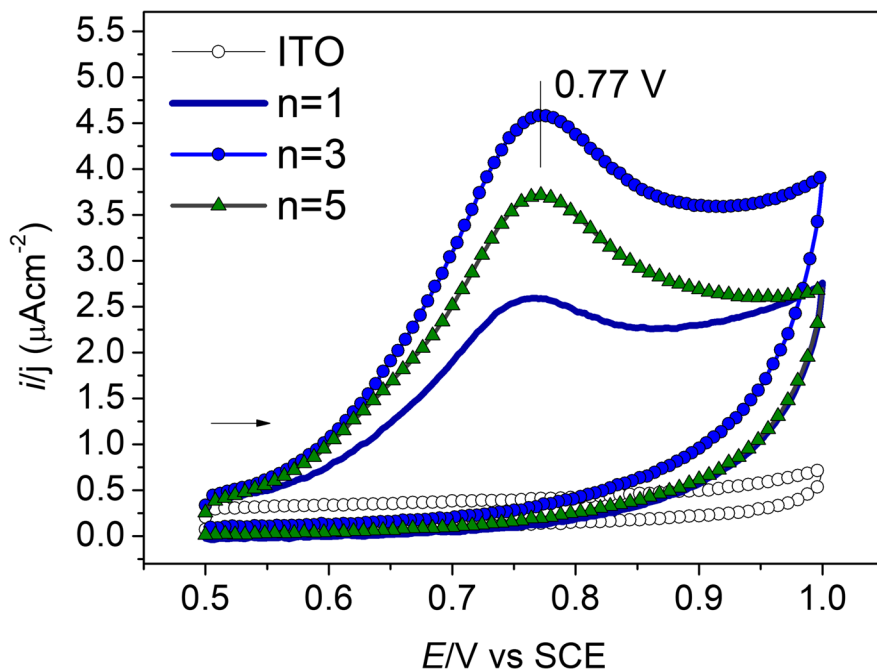


Fig. 5 Cyclic voltammograms for ITO/PIg/DRS 01 with different numbers (n) of bilayers adsorbed. All measurements were performed in phosphate buffer 0.1 mol L^{-1} phosphate buffer, pH 7.25, at 50 mV s^{-1}

Many adsorbed layers hinder the charge transfer to the electrode/electrolyte interface. Because of the results obtained, the ITO/(PIg/DRS 01)₃ film appeared as a new material with potential applications in biotechnology. It was selected for infrared spectroscopy and atomic force microscopy characterization.

In other studies, DRS 01 peptide was immobilized onto cashew gum, a natural polymer (Bittencourt et al., 2016), or on synthetic materials such as tetrasulfonated phthalocyanines (Zampa et al., 2009). Both films exhibited satisfactory results in detecting *Leishmania* cells, also proving the leishmanicidal activity of these materials with different mechanisms observed.

In the present study, the immobilization of DRS 01 in conjunction with PIg allowed the addition of new chemical groups and properties to the film based on this biomolecule. This material may be able to detect other types of pathogens. Because of the antibacterial activity of DRS 01 (Eaton et al., 2014), this perspective of application can be investigated by electrochemistry. Because ITO/PIg/DRS 01 film is a new material, the following steps of this study focused on characterizing it to direct future applications better.

Characterization of LbL Films by UV-Vis

Absorbance analysis in the UV-Vis region allowed us to monitor the growth of the film by measuring light absorption, which is directly related to film thickness. This analysis could indicate the continuity of the formation process of the LbL film after each stage of adsorption.

The growth dependence of ITO/PIg/DRS 01 films on peptide adsorption as a function of the number of bilayers is illustrated in Fig. 6. The insert represents the correlation between absorbance at 280 nm and the number of adsorbed bilayers. A linear increase in absorbance up to the fourth adsorbed bilayer was observed (Fig. 6). The DRS 01 adsorption is believed to occur on the surface and in the microchannels of the PIg fibrous clay. After five bilayers, the maximum incorporation of DRS 01 was reached, as shown by the absorbance saturation observed, and ordered layering begins to fall off. This result supports using the four-bilayer film because it is still in the region of ordered growth. In addition, many LbL films for electrochemical sensing applications in the literature point to four

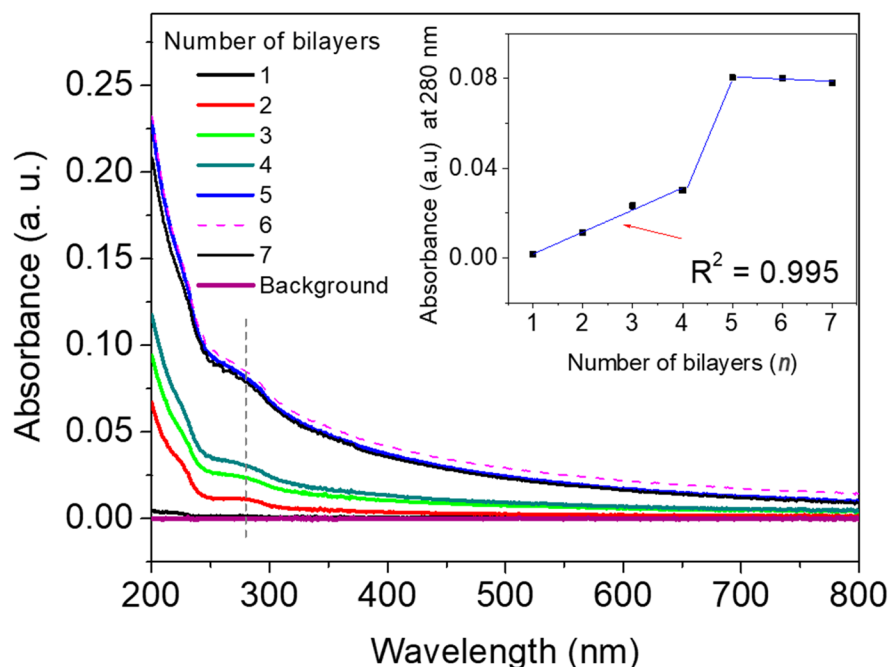


Fig. 6 UV-Vis spectra show the growth of ITO/P1g/DRS 01 with different numbers of bilayers. Insert: the relation between absorbance at 280 nm and the number of adsorbed bilayers

bilayers as the ideal number (Farias et al., 2017; Plácido et al. 2016).

Characterization of LbL Films by Atomic Force Microscopy (AFM)

The deposition technique and materials that influence the morphology and roughness of the thin films were investigated by AFM analysis (Fig. 7). The characteristics observed for ITO used as the control (Fig. 7A) agreed with the AFM analyses reported by Eaton and West (2010), which concluded that the surface consisted of small, globular granules. Concerning the height of the ITO substrate, the value found (51 nm) resembled that reported by Bittencourt et al. (2016). The ITO surface covered with one layer of P1g (Fig 7B) had a more uniform appearance due to the coverage of the interstices and granules in a homogeneous way without producing a change in the height (51 nm).

This result was due to the fine particle-size fraction of P1g obtained by purification, enrichment, and sonication. For the ITO/P1g/DRS01 film with one bilayer (Fig. 7C), its height increased, and

visualization of the cracks decreased slightly. The surface of the ITO/P1g/DRS01 film with three bilayers (Fig. 7D) had a more regular coverage of the granules than the film with one bilayer, with some peaks at the top related to deposition.

Decher and Schlenoff (2012) established that film roughness and uniformity influence directly the formation of the subsequent layer, as well as properties such as thickness, so the surface roughness of the two films was analyzed here (Fig. 8). The average roughness (R_a) value determined by AFM at $4 \mu\text{m} \times 4 \mu\text{m}$ for the ITO was 3.75 ± 0.20 nm. Adding one layer of P1g to the film resulting in virtually no change in roughness (3.62 ± 0.28 nm, with no significant difference at $p < 0.05$) is attributed to the small size of the particles. For the ITO-P1g/DRS 01 film with one bilayer, the change in R_a (3.02 ± 0.48 nm) was significant ($p < 0.05$) when compared to the value found for the ITO. The difference was even greater for the film with three bilayers ($R_a = 4.37 \pm 0.77$ nm) in relation to ITO and other films and, thus, it could be chosen for biotechnological applications.

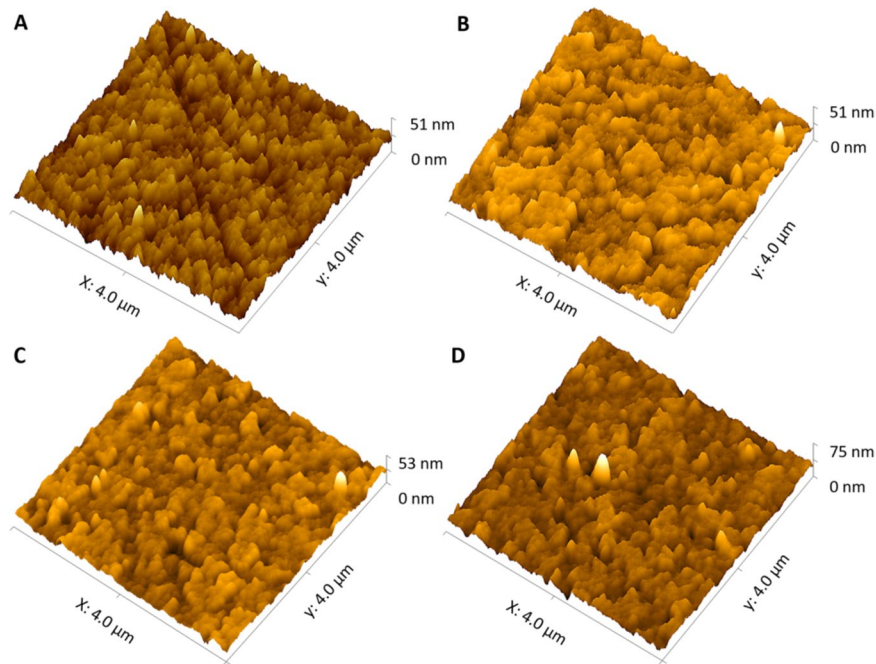


Fig. 7 AFM images of (A) ITO, and ITO coated with (B) ITO/Plg, (C) ITO/(Plg/DRS 01)₁, and (D) ITO/(Plg/DRS 01)₃ (Subscript number refers to the number of bilayers adsorbed on the substrate)

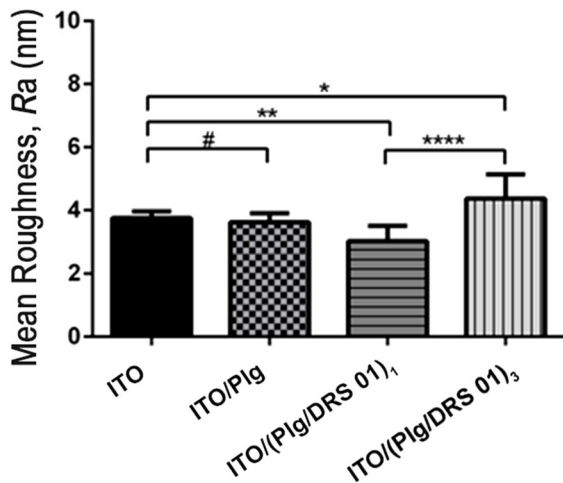


Fig. 8 Comparison of the roughness values (R_a) of the glass surfaces covered with ITO, ITO/Plg, ITO/(Plg/DRS 01)₁, and ITO/(Plg/DRS 01)₃. */**/****: statistically significant differences, #: no statistically significant difference ($n = 10$)

Conclusions

The results indicate that the Plg from Guadalupe in the State of Piauí, Brazil, was purified as confirmed by XRD, FTIR, and CV techniques. This study allowed a new use of raw Plg by improving its characteristics using simple and efficient techniques and a Layer-by-Layer self-assembly process with a biomedically relevant peptide. The LbL films thus obtained can be reproduced even on other substrates due to the good non-covalent interaction between the materials and to the reproducibility of the LbL technique. The purification of clay minerals plays an essential role in the electrode response during cyclic voltammetry. It provides new scientific results, such as its influence on the electrochemical characteristics of the few-layered assemblies. The binding of the DRS 01 peptide to Plg presents opportunities for developing functionalized sensors for rapidly detecting pathogens or treating substrates against biofilm formation with applications in the pharmaceutical, biomedical, and environmental areas. Besides, antimicrobial properties, among other biotechnological applications, can also be explored.

Acknowledgments The authors are grateful to the ‘Coordination of Improvement of Higher-Level Personnel’ (CAPES) for the logistical and financial support and to Katiane C. M. Xavier (CETEM-PI, UESPI) for FTIR measurements of Plg.

Declarations

Conflict of Interest The authors declare no conflict of interest.

References

- Alcântara, A. C. S., Darder, M., Aranda, P., & Ruiz-Hitzky, E. (2012). Zein-fibrous clays biohybrid materials. *European Journal of Inorganic Chemistry*, 32, 5216–5224. <https://doi.org/10.1002/ejic.201200582>
- Alcântara, A. C. S., Darder, M., Aranda, P., & Ruiz-Hitzky, E. (2014). Polysaccharide-fibrous clay bionanocomposites. *Applied Clay Science*, 96, 2–8. <https://doi.org/10.1016/j.clay.2014.02.018>
- Alcântara, A. C. S., Darder, M., Aranda, P., Ayral, A., & Ruiz-Hitzky, E. (2015). Bionanocomposites based on polysaccharides and fibrous clays for packaging applications. *Journal of Applied Polymer Science*, 133, 14p. <https://doi.org/10.1002/app.42362>
- Amiche, M., Ladram, A., & Nicolas, P. (2008). A consistent nomenclature of antimicrobial peptides isolated from frogs of the subfamily Phyllomedusinae. *Peptides*, 29(11), 2074–2082. <https://doi.org/10.1016/j.peptides.2008.06.017>
- An, N., Zhou, C. H., Zhuang, X. Y., Tong, D. S., & Yu, W. H. (2015). Immobilization of enzymes on clay minerals for biocatalysts and biosensors. *Applied Clay Science*, 114, 283–296. <https://doi.org/10.1016/j.clay.2015.05.029>
- Anirudhan, T. S., & Ramachandran, M. (2007). Surfactant-modified bentonite as adsorbent for the removal of humic acid from wastewaters. *Applied Clay Science*, 35, 276–281. <https://doi.org/10.1016/j.clay.2006.09.009>
- Baltar, C. A. M., Luz, A. B., Baltar, L. M., Oliveira, C. H., & Bezerra, F. J. (2009). Influence of morphology and surface charge on the suitability of Palygorskite as drilling fluid. *Applied Clay Science*, 42, 597–600. <https://doi.org/10.1016/j.clay.2008.04.008>
- Bailey, S. W., & Brown, G. (1980). Structure of layer silicates. In: Brindley, G. W., Brown, G. (Eds.) *Crystal structures of clays and their X-ray Identification*. Mineralogical Society, London, pp. 1–123 (Chapter 1). <https://doi.org/10.1180/mono-5>
- Basiuk, V. A., Gromovoy TYu., & Khil’chevskaya, E. G. (1995). Adsorption of small biological molecules on silica from diluted aqueous solutions: quantitative characterization and implications to the Bernal’s hypothesis. Origins of life and evolution of the biosphere. *The Journal of the International Society for the Study of the Origin of Life*, 25(4), 375–393. <https://doi.org/10.1007/BF01581776>
- Belaïd, A., Aouni, M., Khelifa, R., Trabelsi, A., Jemmali, M., & Hani, K. (2002). In vitro antiviral activity of dermaseptins against herpes simplex virus type 1. *Journal of Medical Virology*, 66(2), 229–234. <https://doi.org/10.1002/jmv.2134>
- Belaroui, L. S. Youcef, L. D., & Bengueddach, A. University of Oran. (2014). Mineralogical and Chemical Characterization of Palygorskite from East-Algeria. *Revista de la Sociedad Española de Mineralogía.*, 19, 1–2.
- Benetoli, L. O., de Souza, C. M., da Silva, K. L., de Souza, I. G., Jr, de Santana, H., Paesano, A., Jr, da Costa, A. C., Zaia, C. T., & Zaia, D. A. (2007). Amino acid interaction with and adsorption on clays: FT-IR and Mössbauer spectroscopy and X-ray diffractometry investigations. Origins of life and evolution of the biosphere. *The Journal of the International Society for the Study of the Origin of Life*, 37(6), 479–493. <https://doi.org/10.1007/s11084-007-9072-7>
- Bergaya, F., Theng, B. K. G., & Lagaly, G. (2006). Clays in industry. In F. Bergaya, B. K. G. Theng, & G. Lagaly (Eds.), *Handbook of Clay Science* (Vol. 1, pp. 1–18). Elsevier. (Chapter 1).
- Bittencourt, C. R., de Oliveira Farias, E. A., Bezerra, K. C., Vêras, L. M. C., Silva, V. C., Costa, C. H. N., Bemquerer, M. P., Silva, L. P., de Almeida, Souza, Leite, J. R., & Eiras, C. (2016). Immobilization of cationic antimicrobial peptides and natural cashew gum in nanosheet systems for the investigation of anti-leishmanial activity. *Materials Science & Engineering. C, Materials for Biological Applications*, 59, 549–555. <https://doi.org/10.1016/j.msec.2015.10.059>
- Bourgeois, P. (2006). *El extraordinario poder curativo de la arcilla*. De Vicchi.
- Bradley, W. F. (1940). The structural scheme of attapulgit. *American Mineralogist*, 25, 405–410.
- Brand, G. D., Leite, J. R., Silva, L. P., Albuquerque, S., Prates, M. V., Azevedo, R. B., Carregaro, V., Silva, J. S., Sá, V. C., Brandão, R. A., & Bloch, C., Jr (2002). Dermaseptins from Phyllomedusa oreades and Phyllomedusa distincta. Anti-Trypanosoma cruzi activity without cytotoxicity to mammalian cells. *The Journal of Biological Chemistry*, 277(51), 49332–49340. <https://doi.org/10.1074/jbc.M209289200>
- Brand, G. D., Leite, J. R., de Sá Mandel, S. M., Mesquita, D. A., Silva, L. P., Prates, M. V., Barbosa, E. A., Vinecky, F., Martins, G. R., Galasso, J. H., Kuckelhaus, S. A., Sampaio, R. N., Furtado, J. R., Jr, Andrade, A. C., & Bloch, C., Jr. (2006). Novel dermaseptins from Phyllomedusa hypochondrialis (Amphibia). *Biochemical and Biophysical Research Communications*, 347(3), 739–746. <https://doi.org/10.1016/j.bbrc.2006.06.168>
- Brand, G.D., Santos, R.C., Arake, L.M., Silva, V.G., Veras, L.M.C., Costa, V., Costa, C.H.N., Kuckelhaus, S.S., Alexandre, J.G., Feio, M.J., Leite, J.R.S.A. (2013) The skin secretion of the amphibian Phyllomedusa nordestina: A source of antimicrobial and antiprotozoal peptides. (2013). The skin secretion of the amphibian Phyllomedusa nordestina: A source of antimicrobial and antiprotozoal peptides. *Molecules.*, 18(6), 7058–7070. <https://doi.org/10.3390/molecules18067058>
- Brogden, K. A. (2005). Antimicrobial peptides: pore formers or metabolic inhibitors in bacteria? *Nature Reviews. Microbiology*, 3(3), 238–250. <https://doi.org/10.1038/nrmicro1098>
- Brogden, N. K., & Brogden, K. A. (2011). Will new generations of modified antimicrobial peptides improve their potential as pharmaceuticals? *International Journal of Antimicrobial Agents*, 38(3), 217–225. <https://doi.org/10.1016/j.ijantimicag.2011.05.004>

- Buri, M. V., Domingues, T. M., Paredes-Gamero, E. J., Casasa-Rodrigues, R. L., Rodrigues, E. G., & Miranda, A. (2013). Resistance to degradation and cellular distribution are important features for the antitumor activity of gomesin. *PLoS one*, 8(11), e80924. <https://doi.org/10.1371/journal.pone.0080924>
- Cai, Y., Xue, J., & Polya, D. A. (2007). A Fourier transform infrared spectroscopic study of Mg-rich, Mg-poor and acid leached Palygorskites. *Spectrochimica Acta. Part A, Molecular and Biomolecular Spectroscopy*, 66(2), 282–288. <https://doi.org/10.1016/j.saa.2006.02.053>
- Calderon, L. A., Silva-Jardim, I., & Zuliani, J. P. (2009). Amazonian biodiversity: a view of drug development for Leishmaniasis and Malaria. *Journal of the Brazilian Chemical Society*, 20, 1011–1023. <https://doi.org/10.1590/S0103-50532009000600003>
- Carazo, E., Borrego-Sánchez, A., García-Villén, F., Sánchez-Espejo, R., Viseras, C., Cerezo, P., & Aguzzi, C. (2018). Adsorption and characterization of Palygorskite-isoniazid nanohybrids. *Applied Clay Science*, 160, 180–185. <https://doi.org/10.1016/j.clay.2017.12.027>
- Carretero, M. I. (2002). Clay minerals and their beneficial effects upon human health. A review. *Applied Clay Science*, 21, 155–163. [https://doi.org/10.1016/S0169-1317\(01\)00085-0](https://doi.org/10.1016/S0169-1317(01)00085-0)
- Carretero, M. I., Gomes, C. S. F., & Tateo, F. (2006). Clays and human health. In: Bergaya, F., Theng, B. K. G., Lagaly, G. (Eds.) *Handbook of Clay Science*, Volume 1. Elsevier, Amsterdam, pp. 717–741 (Chapter 11.5).
- Castiglione-Morelli, M. A., Cristinziano, P., Pepe, A., & Temussi, P. A. (2005). Conformation-activity relationship of a novel peptide antibiotic: structural characterization of dermaseptin DS 01 in media that mimic the membrane environment. *Biopolymers*, 80(5), 688–696. <https://doi.org/10.1002/bip.20244>
- Castro-Smirnov, F. A., Ayache, J., Bertrand, J. R., Dardillac, E., Le Cam, E., Aranda, Piétrement., & O., Pilar, A., Ruiz-Hitzky, E., & Lopez, B. S. (2017). Cellular uptake pathways of sepiolite nanofibers and DNA transfection improvement. *Scientific Reports*, 7, 1–10. <https://doi.org/10.1038/s41598-017-05839-3>
- Chahi, A., Petit, S., & Decarreau, A. (2002). Infrared evidence of dioctahedral-trioctahedral site occupancy in Palygorskite. *Clays and Clay Minerals*, 50, 306–313. <https://doi.org/10.1346/00098600260358067>
- Chan, W. C., & White, P. D. (2000). *Fmoc Solid Phase Peptide Synthesis: A Practical Approach*. Oxford Academic, United Kingdom. <https://doi.org/10.1093/oso/9780199637256.001.0001>
- Chen, J., & Jin, Y. (2010). Sensitive phenol determination based on co-modifying tyrosinase and Palygorskite on glassy carbon electrode. *Microchimica Acta*, 169, 249–254. <https://doi.org/10.1007/s00604-010-0320-6>
- Chrzanowski, W., Kim, S. Y., & Neel, E. A. A. (2013). Biomedical applications of clay. *Australian Journal of Chemistry*, 66(11), 1315–1322. <https://doi.org/10.1071/CH13361>
- Chu, H.-L., Yip, B., Chen, K., Yu, H., Chih, Y., Cheng, T., Chou, Y., & Cheng, J. (2015). Novel antimicrobial peptides with high anticancer activity and selectivity. *PLoS ONE*, 10, 1–14. <https://doi.org/10.1371/journal.pone.0126390>
- Costa, F., Carvalho, I. F., Montelaro, R. C., Gomes, P., & Martins, M. C. (2011). Covalent immobilization of antimicrobial peptides (AMPs) onto biomaterial surfaces. *Acta Biomaterialia*, 7(4), 1431–1440. <https://doi.org/10.1016/j.actbio.2010.11.005>
- da Silva, M. L. G., Fortes, A. C., Tomé, A. R., da Silva Filho, E. C., de Freitas, R. M., Soares-Sobrinho, J. L., Leite, C. M. S., & Soares, M. F. L. R. (2013). The effect of natural and organophilic Palygorskite on skin wound healing in rats. *Brazilian Journal of Pharmaceutical Sciences*, 49, 729–736. <https://doi.org/10.1590/S1984-82502013000400012>
- da Silva, M., Fortes, A., Oliveira, M., Freitas, R. M., Soares, M., Sobrinho, J., & Leite, C. (2014). Palygorskite organophilic for dermopharmaceutical application. *Journal of Thermal Analysis and Calorimetry*, 115, 2287–2294. <https://doi.org/10.1007/s10973-012-2891-4>
- de Farias, E. A., Nogueira, O., & S. S., de Oliveira Farias, A. M. (2017). A thin pani and carrageenan-gold nanoparticle film on a flexible gold electrode as a conductive and low-cost platform for sensing in a physiological environment. *Journal of Materials Science*, 52, 13365–13377. <https://doi.org/10.1007/s10853-017-1438-2>
- Decher, G. (1997). Fuzzy Nanoassemblies: Toward layered polymeric multicomposites. *Science*, 277, 1232–1237. <https://doi.org/10.1126/science.277.5330.1232>
- Decher, G., & Schlenoff, J. B. (2012). *Multilayer thin films: sequential assembly of nanocomposite materials* (Vol. 1). Wiley.
- Eaton, P., & West, P. (2010). *Atomic Force Microscopy*. Oxford University Press Inc.
- Eaton, P., Bittencourt, C. R., Costa Silva, V., Vêras, L. M., Costa, C. H., Feio, M. J., & Leite, J. R. (2014). Anti-leishmanial activity of the antimicrobial peptide DRS 01 observed in *Leishmania infantum* (syn. *Leishmania chagasi*) cells. *Nanomedicine: Nanotechnology, Biology, and Medicine*, 10(2), 483–490. <https://doi.org/10.1016/j.nano.2013.09.003>
- Fernandes, F. M., Ruiz, A. I., Darder, M., Aranda, P., & Ruiz-Hitzky, E. (2009). Gelatin-clay bio-nanocomposites: structural and functional properties as advanced materials. *Journal of Nanoscience and Nanotechnology*, 9(1), 221–229. <https://doi.org/10.1166/jnn.2009.j002>
- Gan, F., Zhou, J., Wang, H., Du, C., & Chen, X. (2009). Removal of phosphate from aqueous solution by thermally treated natural Palygorskite. *Water research*, 43(11), 2907–2915. <https://doi.org/10.1016/j.watres.2009.03.051>
- García-Romero, E., Barrios, M. S., & Revuelta, M. A. B. (2004). Characteristics of a Mg-Palygorskite in Miocene rocks, Madrid Basin (Spain). *Clays and Clay Minerals*, 52, 484–494. <https://doi.org/10.1346/CCMN.2004.0520409>
- García-Romero, E., & Suárez, M. (2013). Sepiolite-Palygorskite: textural study and genetic considerations. *Applied Clay Science*, 86, 129–144. <https://doi.org/10.1016/j.clay.2013.09.013>
- Gaspar, D., Veiga, A. S., & Castanho, M. A. (2013). From antimicrobial to anticancer peptides. A review. *Frontiers in Microbiology*, 4, 294. <https://doi.org/10.3389/fmicb.2013.00294>
- Ghadiri, M., Chrzanowski, W., & Rohanizadeh, R. (2015). Biomedical applications of cationic clay minerals. *Royal Society of Chemistry Advances*, 5, 29467–29481. <https://doi.org/10.1039/C4RA16945J>
- Gianfreda, M. A., Rao, F. S., Saccomandi, F., & Violante, A. (2002). Enzymes in soil: properties, behavior and potential applications. *Developments in Soil Science*, 28B, 301–327. [https://doi.org/10.1016/S0166-2481\(02\)80027-7](https://doi.org/10.1016/S0166-2481(02)80027-7)

- Huang, J., Liu, Y., & Wang, X. (2008). Influence of differently modified palygorskites in the immobilization of a lipase. *Journal of Molecular Catalysis B: Enzymatic*, 55, 49–54. <https://doi.org/10.1016/j.molcatb.2007.12.025>
- Huang, J., Liu, Y., & Wang, X. (2009). Silanized Palygorskite for lipase immobilization. *Journal of Molecular Catalysis B: Enzymatic*, 57, 10–15. <https://doi.org/10.1016/j.molcatb.2008.06.009>
- Iborra, C. V., & González, P. C. (2006). Aplicación de peloides y fangos termales. *Técnicas y tecnologías em hidrologia médica e hidroterapia, Madrid.*, 50, 141–146.
- Kim, J. S., Granstrom, M., Amigo, R. H., Johansson, N., Salaneck, W. R., Daik, R., Festa, W. J., & Cacialli, F. (1998). Indium-tin oxide treatments for single- and double-layer polymeric light-emitting diodes: the relation between the anode physical, chemical and morphological properties and /the device performance. *Journal of Applied Physics*, 84, 6859–6870. <https://doi.org/10.1063/1.368981>
- Kim, M. H., Choi, G., Elzatahry, A., Vinu, A., Choy, Y. B., & Choy, J. H. (2016). Review of Clay-Drug Hybrid Materials for Biomedical Applications: Administration Routes. *Clays and Clay Minerals*, 64(2), 115–130. <https://doi.org/10.1346/CCMN.2016.0640204>
- Kong, J., & Yu, S. (2007). Fourier transform infrared spectroscopic analysis of protein secondary structures. *Acta Biochimica et Biophysica Sinica*, 39(8), 549–559. <https://doi.org/10.1111/j.1745-7270.2007.00320.x>
- Lehn, J. M. (2007). From supramolecular chemistry towards constitutional dynamic chemistry and adaptative chemistry. *Chemical Society Reviews*, 36, 151–160. <https://doi.org/10.1039/B616752G>
- Leite, J. R. S. A., Brand, G. D., Silva, L. P., Kückelhaus, S. A. S., Bento, W. R. C., Araújo, A. L. T., Martins, G. R., Lazari, A. M., & Bloch, C., Jr (2008). Dermaseptins from *Phyllomedusa oreades* and *Phyllomedusa distincta*: Secondary structure, antimicrobial activity, and mammalian cell toxicity. *Comparative Biochemistry and Physiology. Part A, Molecular & Integrative Physiology*, 151(3), 336–343. <https://doi.org/10.1016/j.cbpa.2007.03.016>
- Lillehoj, P. B., Kaplan, C. W., He, J., Shi, W., & Ho, C. M. (2014). Rapid, electrical impedance detection of bacterial pathogens using immobilized antimicrobial peptides. *Journal of Laboratory Automation*, 19(1), 42–49. <https://doi.org/10.1177/2211068213495207>
- Liu, Y. F., Huang, J. H., & Wang, X. G. (2008). Adsorption isotherms for bleaching soybean oil with activated attapulgite. *Journal of the American Oil Chemists' Society*, 85, 979–984. <https://doi.org/10.1007/s11746-008-1278-y>
- López-Galindo, A., Viseras, C., & Cerezo, P. (2007). Compositional, technical and safety specifications of clays to be used as pharmaceutical and cosmetic products. *Applied Clay Science*, 36, 51–63. <https://doi.org/10.1016/j.clay.2006.06.016>
- Madejová, J., & Komadel, P. (2001). Baseline studies of the Clay Minerals Society Source Clays: Infrared methods. *Clays and Clay Minerals*, 49, 410–432. <https://doi.org/10.1346/CCMN.2001.0490508>
- Madyan, O. A., Fan, M., & Huang, Z. (2017). Functional clay aerogel composites through hydrophobic modification and architecture of layered clays. *Applied Clay Science*, 141, 64–71. <https://doi.org/10.1016/j.clay.2017.01.013>
- Mbougou, J. K., Ngameni, E., & Walcarius, A. (2006). Organoclay-enzyme film electrodes. *Analytica Chimica Acta*, 578(2), 145–155. <https://doi.org/10.1016/j.aca.2006.06.075>
- Mbougou, J. K., Ngameni, E., & Walcarius, A. (2007). Quaternary ammonium functionalized clay film electrodes modified with polyphenol oxidase for the sensitive detection of catechol. *Biosensors and Bioelectronics*, 23, 269–275. <https://doi.org/10.1016/j.bios.2007.04.008>
- Mor, A., Hani, K., & Nicolas, P. (1994). The vertebrate peptide antibiotics dermaseptins have overlapping structural features but target specific microorganisms. *The Journal of Biological Chemistry*, 269(50), 31635–31641.
- Moraes, J., Nascimento, C., Miura, L. M. C. V., Leite, J. R. S. A., Nakano, E., & Kawano, T. (2011). Evaluation of the *in vitro* activity of Dermaseptin 01, a cationic antimicrobial peptide, against *Schistosoma mansoni*. *Chemistry & Biodiversity*, 8, 548–558.
- de Moraes, J., Nascimento, C., Miura, L. M., Leite, J. R., Nakano, E., & Kawano, T. (2011). Evaluation of the *in vitro* activity of dermaseptin 01, a cationic antimicrobial peptide, against *Schistosoma mansoni*. *Chemistry & Biodiversity*, 8(3), 548–558. <https://doi.org/10.1002/cbdv.201000163>
- Mousty, C. (2004). Sensors and biosensors based on clay-modified electrodes – new trends. *Applied Clay Science*, 27, 159–177. <https://doi.org/10.1016/j.clay.2004.06.005>
- Murray, H. H. (2007). Applied clay mineralogy, occurrences, processing and application of kaolins, bentonites, palygorskite-sepiolite, and common clays. *Developments in Clay Science*, 2, Elsevier, Amsterdam, 188 pp.
- Navrátilová, Z., & Kula, P. (2003). Clay modified electrodes: present applications and prospects. *Electroanalysis*, 15, 837–846. <https://doi.org/10.1002/elan.200390103>
- Ntwasa, M. (2012). Cationic peptide interactions with biological macromolecules. In: Abdelmohsen, K. (Ed.). *Binding Protein. InTechOpen*, Rijeka. pp. 139-164 (Chapter 6). <https://doi.org/10.5772/48492>
- Oliveira, A. M. B. M., Coelho, L. F. O., Gomes, S. S. S., Costa, I. F., Fonseca, M. G., Sousa, K. S., Espínola, J. G. P., & Filho, E. C. S. (2013). Brazilian palygorskite as adsorbent for metal ions from aqueous solution-kinetic and equilibrium studies. *Water, Air, & Soil Pollution*, 224, 1–12. <https://doi.org/10.1007/s11270-013-1687-x>
- Onaizi, S. A., & Leong, S. S. (2011). Tethering antimicrobial peptides: current status and potential challenges. *Biotechnology Advances*, 29(1), 67–74. <https://doi.org/10.1016/j.biotechadv.2010.08.012>
- Plgeček, E., Tkáč, J., Bartošík, M., Bertók, T., Ostatná, V., & Plgeček, J. (2015). Electrochemistry of nonconjugated proteins and glycoproteins. Toward sensors for biomedicine and glycomics. *Chemical Reviews*, 115(5), 2045–2108. <https://doi.org/10.1021/cr500279h>
- Parbhakar, A., Cuadros, J., Sephton, M. A., Dubbin, W., Coles, B. J., & Weiss, D. (2007). Adsorption of l-lysine on montmorillonite. *Colloids and Surfaces A*, 307, 142–149. <https://doi.org/10.1016/j.colsurfa.2007.05.022>
- Picart, C., Caruso, F., Voegel, J., & Decher, G. (2015). *Layer-by-layer Films for Biomedical Applications*. Wiley.
- Plácido, A., de Oliveira Farias, E. A., Marani, M. M., Vasconcelos, A. G., Mafud, A. C., Mascarenhas, Y. P., Eiras, C., Leite, J. R., & Delerue-Matos, C. (2016). Layer-by-layer films containing peptides of the Cry1Ab16 toxin from

- Bacillus thuringiensis for potential biotechnological applications. *Materials Science & Engineering. C, Materials for Biological Applications*, 61, 832–841. <https://doi.org/10.1016/j.msec.2016.01.011>
- Rawtani, D., & Agrawal, Y. K. (2014). Emerging strategies and applications of layer-by-layer self-assembly. *Nanobiomedicine*, 1, 1–15. <https://doi.org/10.5772/60009>
- Romero, E. G., & Barrios, M. S. (2008). Sobre la composición química de sepiolita y Palygorskita. *Revista de la Sociedad Española de Mineralogía*, 9, 111–112.
- Ruiz-Hitzky, E., & Van Meerbeek, A. (2006). Clay mineral– and organoclay–polymer nanocomposites. In: Bergaya, F., Theng, B. K. G., Lagaly, G. (Eds.) *Handbook of Clay Science*, Elsevier, Volume 1, Amsterdam, pp. 583–621 (Chapter 10.3).
- Ruiz-Hitzky, E., Darder, M., Fernandes, F. M., Wicklein, B., Alcántara, A. C. S., & Aranda, P. (2013). Fibrous clays based bionanocomposites. *Progress in Polymer Science*, 38, 1392–1414. <https://doi.org/10.1016/j.progpolymsci.2013.05.004>
- Salay, L. C., Nobre, T. M., Colhone, M. C., Zanicuelli, M. E., Ciancaglini, P., Stabeli, R. G., Leite, J. R., & Zucolotto, V. (2011). Dermaseptin 01 as antimicrobial peptide with rich biotechnological potential: study of peptide interaction with membranes containing Leishmania amazonensis lipid-rich extract and membrane models. *Journal of Peptide Science: An Official Publication of the European Peptide Society*, 17(10), 700–707. <https://doi.org/10.1002/psc.1392>
- Sheng, J., & Wang, L. (2005). Preparation and properties of polypropylene/org-attapulgite nanocomposites. *Polymer*, 46, 6243–6249. <https://doi.org/10.1016/j.polymer.2005.05.067>
- Silva, L. P., Leite, J. R. S. A., Brand, G. D., Regis, W. B., Tedesco, A. C., Azevedo, R. B., Freitas, S. M., & Bloch, C., Jr (2008). Dermaseptins from Phyllomedusa oreades and Phyllomedusa distincta: liposomes fusion and/or lysis investigated by fluorescence and atomic force microscopy. Comparative biochemistry and physiology. *Comparative Biochemistry and Physiology Part A: Molecular & Integrative Physiology* 151(3), 329–335. <https://doi.org/10.1016/j.cbpa.2007.02.031>
- Skorb, E. V., Volkova, A. V., & Andreeva, D. V. (2014). Layer-by-layer assembled hybrid materials for sustainable applications. *Current Organic Chemistry*, 18, 2315–2333. <https://doi.org/10.2174/1385272819666140806200646>
- Suárez, M., & García-Romero, E. (2006). FTIR spectroscopic study of palygorskite: influence of the composition of the octahedral sheet. *Applied Clay Science*, 31, 154–163. <https://doi.org/10.1016/j.clay.2005.10.005>
- Suárez, M., & García-Romero, E. (2006). Macroscopic palygorskite from Lisbom volcanic complex. *European Journal of Mineralogy*, 18, 119–126. <https://doi.org/10.1127/0935-1221/2006/0018-0119>
- Suárez, M., García-Romero, E., Del Río, M. S., Martinetto, P., & Dooryhée, E. (2007). The effect of the octahedral cations on the dimensions of the palygorskite cell. *Clay Minerals*, 42, 287–297. <https://doi.org/10.1180/claymin.2007.042.3.02>
- Stucki, J. W. (2006). Properties and behavior of iron in clay minerals. In: Bergaya, F., Theng, B. K. G., Lagaly, G. (Eds.) *Handbook of Clay Science*. Elsevier, vol 1, Amsterdam, pp. 423–475 (Chapter 8).
- Tajeu, K. Y., Ymele, E., Jiokeng, S. L. Z., & Tonle, I. K. (2018). Electrochemical sensor for caffeine based on a glassy carbon electrode modified with an attapulgite/nafion film. *Electroanalysis*, 30, 1–8. <https://doi.org/10.1002/elan.201800621>
- Wang, W., & Wang, A. (2016). Recent progress in dispersion of palygorskite crystal bundles for nanocomposites. *Applied Clay Science*, 119, 18–30. <https://doi.org/10.1016/j.clay.2015.06.030>
- Wu, P., Cai, Z., Chen, J., Zhang, H., & Cai, C. (2011). Electrochemical measurement of the flux of hydrogen peroxide releasing from RAW 264.7 macrophage cells based on enzyme-attapulgite clay nanohybrids. *Biosensors & Bioelectronics*, 26(10), 4012–4017. <https://doi.org/10.1016/j.bios.2011.03.018>
- Xavier, K. C. M., Santos, M. S. F., Osajima, J. A., Luz, A. B., Fonseca, M. G., & Silva Filho, E. C. (2016). Thermally activated palygorskites as agents to clarify soy. *Applied Clay Science*, 119, 338–347. <https://doi.org/10.1016/j.clay.2015.10.037>
- Yan, W., Liu, D., Tan, D., Yuan, P., & Chen, M. (2012). FTIR spectroscopy study of the structure changes of palygorskite under heating. *Spectrochimica Acta. Part A, Molecular and Biomolecular Spectroscopy*, 97, 1052–1057. <https://doi.org/10.1016/j.saa.2012.07.085>
- You, Q., Yin, X., Gu, X., Xu, H., & Sang, L. (2011). Purification, immobilization and characterization of linoleic acid isomerase on modified palygorskite. *Bioprocess and Biosystems Engineering*, 34(6), 757–765. <https://doi.org/10.1007/s00449-011-0525-z>
- Zaia, D. A. (2004). A review of adsorption of amino acids on minerals: was it important for origin of life? *Amino Acids*, 27(1), 113–118. <https://doi.org/10.1007/s00726-004-0106-4>
- Zampa, M. F., Araújo, I. M., Costa, V., Nery Costa, C. H., Santos, J. R., Jr, Zucolotto, V., Eiras, C., & Leite, J. R. (2009). Leishmanicidal activity and immobilization of dermaseptin 01 antimicrobial peptides in ultrathin films for nanomedicine applications. *Nanomedicine: Nanotechnology, Biology, and Medicine*, 5(3), 352–358. <https://doi.org/10.1016/j.nano.2008.11.001>
- Zhao, G., Wang, J., Li, Y., Chen, X., & Liu, Y. (2011). Enzymes immobilized on superparamagnetic Fe₃O₄@clays nanocomposites: preparation, characterization, and a new strategy for the regeneration of supports. *The Journal of Physical Chemistry C*, 115, 6350–6359. <https://doi.org/10.1021/jp200156j>

Springer Nature or its licensor (e.g. a society or other partner) holds exclusive rights to this article under a publishing agreement with the author(s) or other rightsholder(s); author self-archiving of the accepted manuscript version of this article is solely governed by the terms of such publishing agreement and applicable law.